

# Experimental Study on Two-Phase Flow in Horizontal Tube Bundle Using SF6-Water

**ISHIKAWA Atsushi** : Heat & Fluid Dynamics Department, Research Laboratory, Corporate Research & Development

**IMAI Ryoji** : Doctor of Engineering, Manager, Heat & Fluid Dynamics Department, Research Laboratory, Corporate Research & Development

**TANAKA Takahiro** : Ph. D., Manager, Project Management Department, Project Center, Energy & Plant Operations

This study focuses on evaluating constitutive equation of two-phase flow drift flux model under horizontal tube bundle. In two-phase flow, liquid to gas density ratio is one of the most important parameters to simulate the flow structure. Sulfur hexafluoride (SF6) gas and water were used to simulate water-vapor two-phase flow behavior of PWR steam-generator at ambient temperature and low pressure under 1 MPa. The test section consists of a 360 mm high rectangular channel of  $150.9 \times 160$  mm with square pitch horizontal tube bundle of 8 rows of 5 tubes. Each tube has 22.23 mm outer diameter and arranged in line with a pitch of 32.54 mm. Pitch-to-diameter ratio  $P/D$  is 1.46. The experiments were conducted at 0.4 to 0.6 MPa<sub>abs</sub> and ambient temperature. The superficial velocity of SF6 gas and water at the tube gap were changed in the range  $j_G = 1.5$  to 13.5 m/s and  $j_L = 1.2$  to 2.4 m/s, respectively. Time averaged void fraction and interfacial gas velocity was measured using Bi-Optical Probe (BOP). These results were compared with the values generated by previous empirical equations to verify soundness of this facility and measurement method.

## 1. Introduction

Gas-liquid two-phase flow is applied to many industrial products such as Pressurized Water Reactor (PWR) steam-generator, various types of industrial boiler, heat exchanger, and so on. It is well known that two-phase flow behavior is strongly influenced by the flow condition and geometric configuration of the flow region. Therefore, it is important to know the flow structure of those products for their designing, development, and estimating their performance. To improve prediction of two-phase flow, experimental data of each geometric configuration is needed to obtain the constitutive equation. However, it is difficult to measure two-phase flow parameters in many cases, because those products are used under high pressure and high temperature conditions. Flow induced vibration in the case of gas-liquid two-phase flow is one of the most important and complicated issue which occurs mainly at the tube bundle under the cross flow condition. In order to conduct safety design of the industrial products and estimate their performance, evaluation of prediction accuracy of the simulation code in which constitutive equations are used is needed. To simulate two-phase flow behavior, liquid to gas density ratio, liquid to gas viscosity ratio, and surface tension are the important parameters. Among them, the liquid to gas density ratio and the surface tension are the more important parameters. Surface tension is important to simulate the bubble sizes and its shapes, however it is very difficult to treat both the liquid to gas density ratio

and the surface tension arising in the tests the same as those arising in the operation actual products because of several restrictions in carrying out this experiment. Therefore, the liquid to gas density ratio was given higher priority over the surface tension. Several researchers have reported on simulation of two-phase flow behavior of actual products at comparatively low pressure and low temperature.<sup>(1), (2)</sup> In this study, sulfur hexafluoride (SF6) gas and water were used to simulate water-vapor two-phase flow behavior of the industrial products at ambient temperature and low pressure below 1 MPa. Void fraction and gas-liquid interfacial velocity at the horizontal tube bundle were measured in this test facility.

## 2. Experiment

### 2.1 Experimental apparatus

**Figure 1** shows a schematic diagram of the experimental apparatus. The working fluid comprises water for the liquid phase and SF6 gas for the gas phase. Owing to its approximate density of five times that of air, SF6 gas under relatively low pressure can reproduce a gas-liquid density ratio equivalent to the density ratio of high-temperature and high-pressure steam and water. Two SF6 tanks with a capacity of 1 m<sup>3</sup> each were installed for adjusting the pressure inside the loop of the experimental apparatus and collecting SF6 gas.

The flow of the working fluid is described as follows. SF6 gas and water are gravitationally separated in the gas-liquid separator. After being pressurized by the circulation

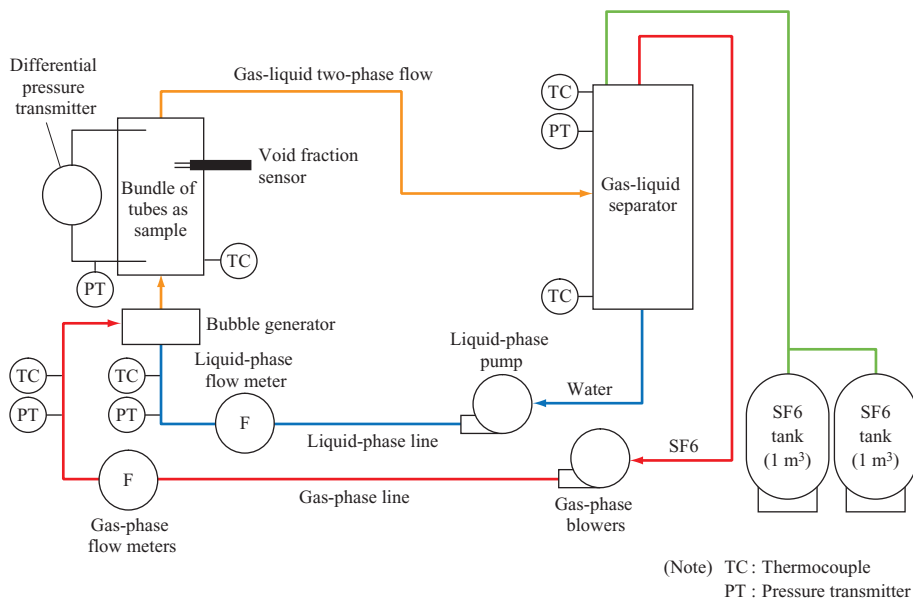


Fig. 1 Schematic diagram of experimental apparatus

pump (vortex pump: 37 kW), the water forms an upward flow from beneath the test section through the flow meter to return to the gas-liquid separator. On the other hand, SF6 gas is pressurized by the electric blower (9 kW × 4 units) and is supplied to the bubble generator through four ports after passing through the flow meter.

**Figure 2** illustrates the structure of the bubble generator. In the bubble generator, part of the wall of the piping for the liquid phase is made of metal gauze, which is surrounded by a donut-shaped chamber. Here, SF6 gas supplied to the chamber is introduced to the liquid phase tube from the periphery. In addition, a check valve is installed between the bubble generator and flow meter to prevent the back flow of water into the gas phase tube. Water and SF6 gas mixed in the bubble generator pass through the metal gauze, which is being used as a flow straightener, and the test section. Finally, the two-phase flow returns to the gas-liquid separator. An orifice flow

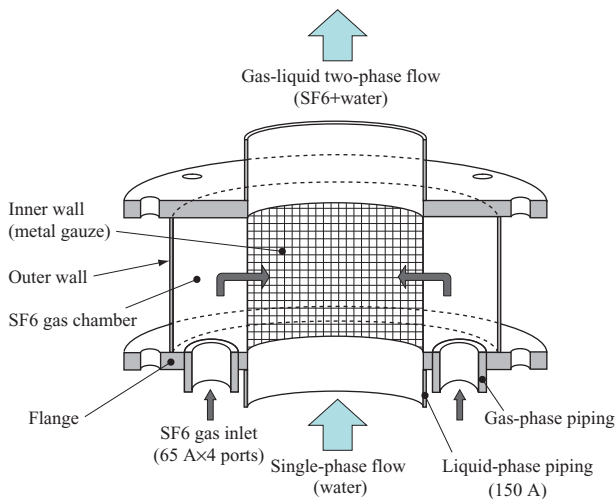


Fig. 2 Structure of bubble generator

meter situated below the test section was used for both the liquid phase and the gas phase.

The maximum volumetric flow rate in this experimental apparatus is approximately 5 m<sup>3</sup>/min for the gas phase and 1 m<sup>3</sup>/min for the liquid phase. Considering the additional pressure corresponding to the hydraulic head in comparison to the pressure of the test section, the volumetric flow rate of the gas flow running through the test section was obtained from the value measured by the orifice flow meter after correcting it in consideration of the test section pressure. The cross-sectional shape of the flow path for the test section is a rectangle with dimensions of 150.9 × 160.0 mm. **Figure 3** shows the alignment of the bundle of horizontal tubes that runs through the test section.

The test section is composed of horizontal tubes that are aligned in five columns (across the width of the vertical flow path) and eight rows (along the flow) whose outer diameter ( $D$ ) is 22.23 mm and pitch ( $P$ ) is 32.54 mm ( $P/D = 1.46$ ) enclosed in the channel of 150.9 × 160 mm rectangular cross-section and 360 mm high. With reference to **Fig. 3**, single-tip electrical resistivity void sensor were mounted on the spots marked with x's (outer diameter: 0.2 mm) and a Bi-Optical Probe (BOP) was mounted on the spot marked with a ♦.

These two different kinds of probes which work based on distinct principles for measuring void fraction were used to validate the measurement method. Optical probes are highly sensitive, although expensive and fragile, thus demanding utmost care in their handling. In contrast, electrical resistivity void sensor, though not applicable to nonconductive fluids, are most commonly used for locally measuring two-phase flows owing to the high degree of flexibility that enables users to build their own low-cost and robust sensors.

**Figure 4** shows a window for observing the internal flow of the test section. More specifically, the figure makes

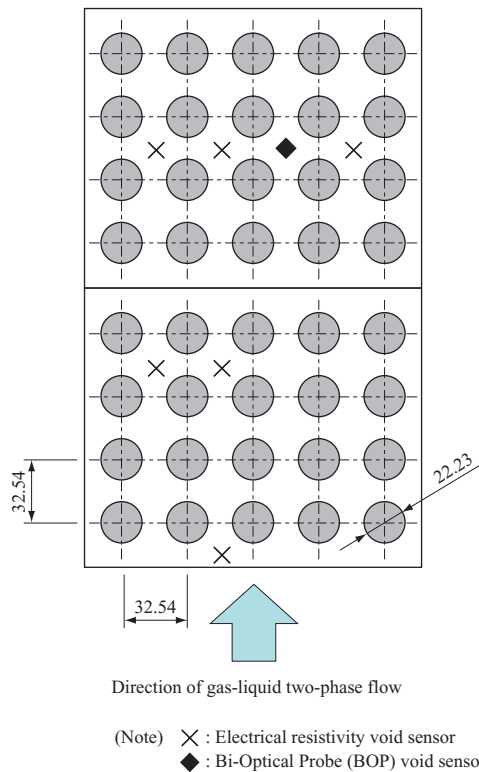


Fig. 3 Schematic diagram of test section (unit: mm)

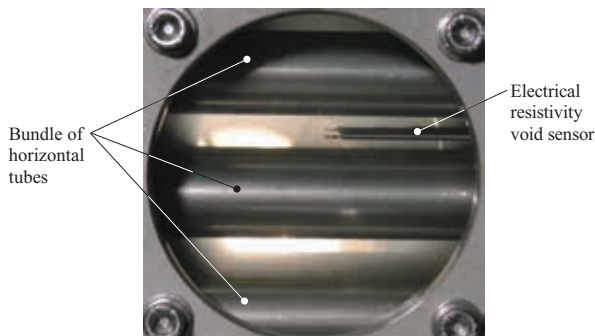
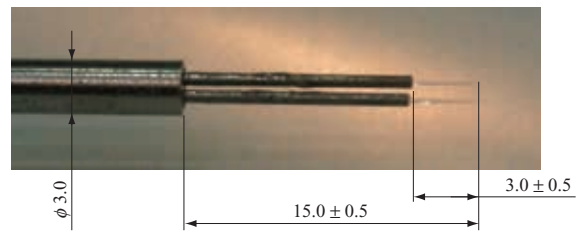


Fig. 4 Observation window of test section

tubes visible from the fifth to seventh columns. **Figure 5** shows the BOP (diameter at the tip <math>< 50 \mu\text{m}</math>) and electrical resistivity void sensor. The single-tip electrical resistivity void sensors detect the difference in conductivities of the gas phase and liquid phase and are used only for measuring the void fraction,<sup>(3)</sup> whereas the BOP detects the difference in refractive indices of the gas phase and liquid phase and

(a) Bi-Optical Probe (BOP) void sensor



(b) Electrical resistivity void sensor (made by IHI)



Fig. 5 Picture of void sensor (unit:mm)

is used for measuring both the void fraction and the gas-liquid interface velocity. In the BOP, local time average void fraction is calculated according to the threshold value determined on the basis of the difference in the voltages corresponding to the gas phase and the liquid phase after converting the optical signals to voltage values using an amplifier and an opto-electronic transformation.

Besides, the gas-liquid interface velocity is derived by dividing the distance between the two probe tips by the time lag of the two output signal waveforms. The time lag is the reading of the traveling time of the gas-liquid interface in the cross-correlation function<sup>(4)</sup> obtained from the time-shifted output signal waveforms from the sensor.

## 2.2 Experimental conditions

**Tables 1** and **2** respectively show the gas-liquid density ratio of the test section and the experimental conditions. In the **Table 1**, the gas-liquid density ratio of water and SF6 gas at 0.6 MPa<sub>abs</sub> corresponds to the actual steam generator. The similar gas-liquid density ratio was used as the experimental condition by the Commissariat à l'énergie atomique (CEA) of France, which is used as reference for comparison with the results of this experiment in a later section.<sup>(1)</sup> The superficial velocity derived by dividing the volumetric flow rate with the minimum cross-sectional area between tubes in the flow path left by the tubes is 1.5 to 13.5 m/s in the gas phase and 1.2 to 2.4 m/s in the liquid

Table 1 Liquid-gas density ratio of working fluid

Item	Unit	Actual PWR's SG		Experimental apparatus (by IHI)		Experimental apparatus (by CEA)	
		Water	Water	Water	Water		
Fluid	Liquid phase	—	Water	Water	Water	Freon-114	
	Gas phase	—	Steam	Steam	SF6	Freon-114 vapor	
	Pressure	MPa <sub>abs</sub>	5.3	6.2	0.4	0.6	0.9
	Temperature	°C	267.58	277.70	20	20	78.50
Density	Liquid phase	kg/m <sup>3</sup>	771.76	754.60	998.46	998.55	1 267.70
	Gas phase	kg/m <sup>3</sup>	26.98	31.95	25.21	38.90	65.75
Gas-liquid density ratio	—	28.61	23.62	39.60	25.67	19.28	

Table 2 Experimental conditions

Item	Unit	Case 1	Case 2
Pressure	MPa <sub>abs</sub>	0.4	0.6
Temperature	°C	20	20
Gas-liquid density ratio	—	39.6	25.7
Superficial velocity of gas phase	m/s	2.2 to 15.8	1.5 to 11.2
Superficial velocity of liquid phase	m/s	1.2 to 2.4	1.2 to 2.4

phase. The gas-liquid density ratios in case 1 and case 2 respectively correspond to steam-water density ratios at saturation temperature which is 250°C under 4.0 MPa<sub>abs</sub> and 271°C under 5.6 MPa<sub>abs</sub>.

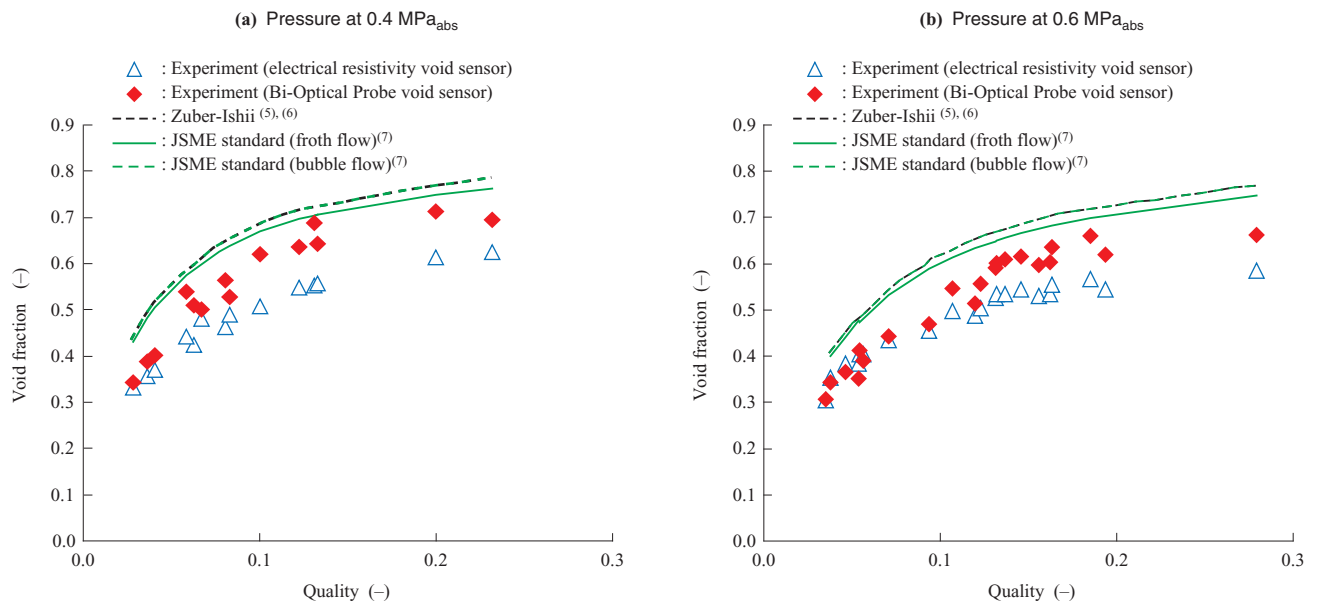
### 3. Results and discussion

**Figure 6** compares the profile of void fraction versus the quality as measured in this experiment and as calculated from the empirical correlation. The horizontal axis in the figure represents the quality. The experiment results are plotted and the estimation values according to the correlation of the drift flux model<sup>(5)-(7)</sup> are drawn as lines.

**Table 3** presents the distribution functions  $C_0$  and drift velocities  $V_{Gj}$  needed for deriving the void fraction based on the drift flux model. Due to lack of an experimental equation based on sufficient results of experiments with bundles of tubes, comparison was made with an empirical correlation used for a single round tube. As a result the profiles of the void fraction correspond to the increase in

the quality in a qualitative manner. An excellent match was observed between the values measured by using electrical resistivity void sensors and values using a BOP, particularly in the low range of quality, validating the void fraction measurement method. However, an increasingly large gap emerges between the two in the higher range of quality. One of the reason is that the electrical resistivity void sensor and its circuitry is built from scratch, which has the disadvantage of inferior responsiveness as compared to the optical sensor.

As shown in **Fig. 6**, all the results from this experiment marked lower values than those obtained from the correlation of the drift flux model. The measurement point of the void fraction is situated at the center of the four tubes as illustrated in **Fig. 7**. This figure explains that bubbles are captured in the trailing vortex between the tubes in the direction of flow. This may be the reason for the relatively low void fraction at the measurement point. Change in the distribution of void fraction as a result of the trailing vortex

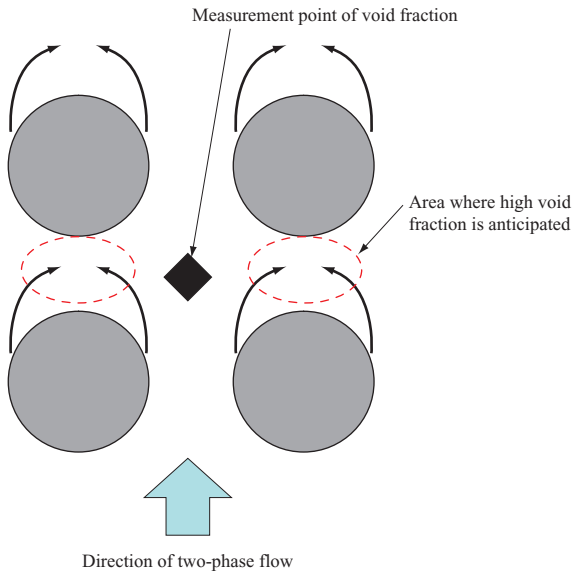


**Fig. 6** Relationship between quality and void fraction at the test section

**Table 3** Parameters of drift flux model

Item	Distribution function $C_0$	Drift velocity $V_{Gj}$
Zuber-Ishii <sup>(5),(6)</sup>	$\left(1.2 - 0.2 \sqrt{\frac{\rho_G}{\rho_L}}\right) \cdot (1 - e^{-18/\alpha})$	$\sqrt{2} \left\{ \frac{\sigma g (\rho_L - \rho_G)}{\rho_L^2} \right\}^{1/4}$
JSME standard (froth flow) <sup>(7)</sup>	1.2	$0.35 \left\{ \frac{g D (\rho_L - \rho_G)}{\rho_L} \right\}^{1/2}$
JSME standard (bubble flow) <sup>(7)</sup>	$1.2 - 0.2 \sqrt{\frac{\rho_G}{\rho_L}}$	$\sqrt{2} \left\{ \frac{\sigma g (\rho_L - \rho_G)}{\rho_L^2} \right\}^{1/4}$

(Note)  $\rho_G$  : gas-phase density  
 $\rho_L$  : liquid-phase density  
 $\alpha$  : void fraction  
 $\sigma$  : surface tension  
 $g$  : gravitational acceleration  
 $D$  : hydraulic equivalent diameter  
 $\langle \rangle$  : Average value of cross section



**Fig. 7** Measurement point of void fraction within the tube bundle

was also reported in the experiment conducted by the CEA.<sup>(1)</sup>

The images of two-phase flow running through a bundle of horizontal tubes are presented in **Fig. 8**. The images were taken with a system pressure of 0.6 MPa<sub>abs</sub>, superficial velocity in the liquid phase ( $j_L$ ) of 1.6 m/s, and superficial


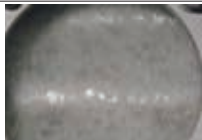
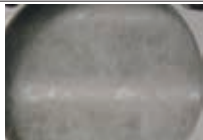
velocity in the gas phase ( $j_G$ ) of 1.6, 4.8 and 7.8 m/s (quality: 0.04, 0.11 and 0.16). These still images were captured from the video recorded by a camcorder at a frame rate of 30 fps and a shutter speed of 1/1 000 s.

In these images, numerous microscopic rising bubbles were observed. Although detailed behavior of the bubbles is unclear because of the small frame rate of the recording device and the limitation in capturing clear images in relation to the speed of two-phase flow under the experimental conditions.

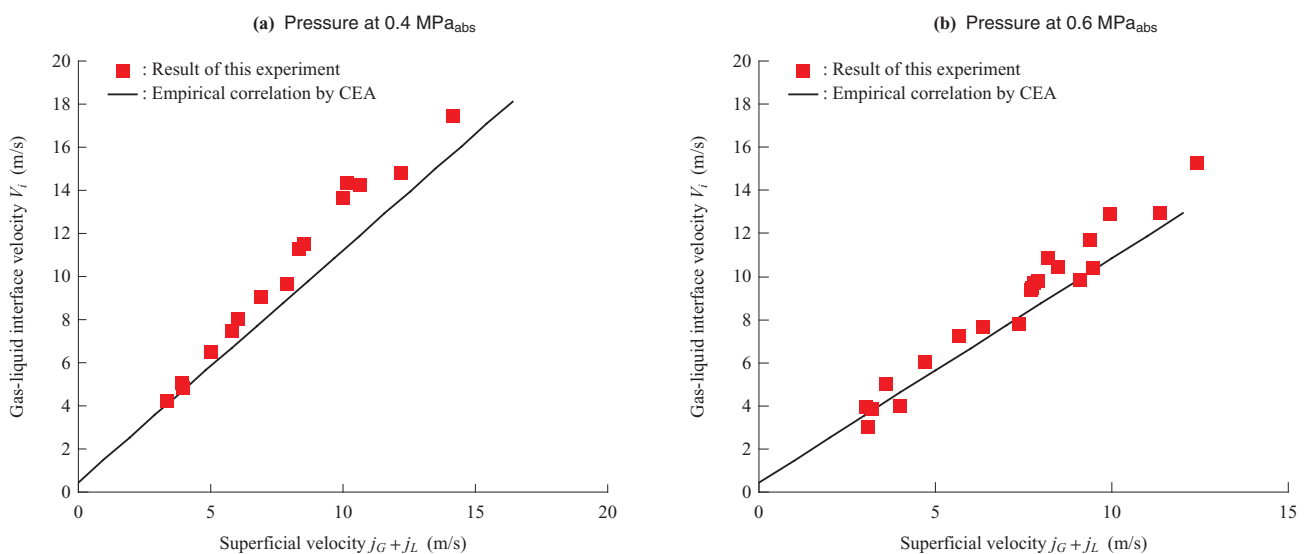
But if nothing else, the change of the blur of bubbles in motion in response to the increase in quality can be visually confirmed.

The change in the measured void fraction in the bundle of tubes from around 0.3 in **Fig. 8-(a)** to over 0.5 in **Figs. 8-(b)** and **-(c)** plausibly suggests the transition to a slug flow, froth flow, or churn flow. The tendency of visibly lower void fraction near the wall and higher void fraction at the center of the flow path has already been found in previous research reported by other research teams. Therefore the same tendency was observed in this experiment.

**Figure 9** presents the profile of the gas-liquid interface velocity along the vertical axis versus total superficial velocity of both the gas phase and the liquid phase along the horizontal axis. The distribution function of the drift

Item		(a)	(b)	(c)
System pressure	(MPa <sub>abs</sub> )	0.6	0.6	0.6
$j_L$ : Superficial velocity of liquid phase	(m/s)	1.6	1.6	1.6
$j_G$ : Superficial velocity of gas phase	(m/s)	1.6	4.8	7.8
$X$ : Quality	(-)	0.04	0.11	0.16
Image of two-phase flow				

**Fig. 8** Image of two-phase flow at the test section



**Fig. 9** Relationship between superficial velocity and interfacial velocity

flux model and drift velocity can be obtained by least squares straight-line approximation. The relational equation (1) applied in the drift flux model is as follows:

$$V_i = C_0(j_G + j_L) + V_{Gj} \quad \text{.....(1)}$$

wherein:

$V_i$  : Gas-liquid interface velocity

$C_0$  : Distribution function

$j_G$  : Superficial velocity in the gas phase

$j_L$  : Superficial velocity in the liquid phase

$V_{Gj}$  : Drift velocity

In addition, as a reference for comparison, the result based on the empirical correlation derived from the experiment by the CEA is presented in **Fig. 9**. The empirical correlation by the CEA is derived by an experiment involving the boiling Measurement point of void fraction of Freon 114 (chlorofluorocarbon) as the working fluid. In this experiment the pressure applied in the experiment was approximately 0.9 MPa while the gas-liquid density ratio was 19.3. A good agreement was observed between the result of this experiment and the existing empirical correlation obtained in the experiment conducted by the CEA with the similar gas-liquid density ratio, wherein the error was less than 10%.

The good agreement between the result of this adiabatic two-phase flow experiment and the empirical correlation of the CEA's boiling experiment validated the effectiveness of simulating a boiling two-phase flow with an adiabatic twophase flow experiment even in the developed two-phase area where there is no transition of the flow regime along the flow.

#### 4. Conclusion

An adiabatic two-phase flow experiment was conducted by making an experimental apparatus, which can reproduce the gas-liquid density ratio of high-temperature high-pressure water and steam at room temperature under a pressure of 1 MPa or less. Comparison of the result of this experiment with the existing empirical correlation demonstrated a good agreement between the two with an error of less than 10%, which validates the integrity of the experimental apparatus, as well as the measurement method. Nevertheless, the data on gas-liquid interface velocity was collected from only one measurement point located at the center of the flow path. We are therefore moving ahead with the plan to make up for the shortfall in the measurement points by

obtaining further data of the cross-sectional distribution of void fraction in the flow path and the distribution of flow velocity.

#### — Acknowledgements —

The valuable advice of Professor Isao Kataoka and Associate Professor Kenji Yoshida from the Department of Mechanical Engineering, Graduate School of Engineering, Osaka University was instrumental in making the electrical resistivity void sensor for the experimental apparatus for this study. We take this opportunity to gratefully express our appreciation.

#### REFERENCES

- (1) J. F. Haquet and J. M. Gouirand : Local Two-Phase Flow Measurements in a Cross-Flow Steam-Generator Tube Bundle Geometr : The Minnie II XF Program Proc. of International Multiphase Flow (1995) p. TT-17
- (2) T. Suzuta, T. Ueno, Y. Hirao, K. Tomomatsu, K. Kawanishi and A. Tsuge : Measurement of Interfacial Velocities in Gas-Liquid Upward Two-Phase Flow across Tube Bundle 7th International Conference on Nuclear Engineering ICONE-7483 (1999. 4) pp. 1-9
- (3) Atomic Energy Society of Japan (AESJ) : ADVANCED MEASUREMENT IN MULTIPHASE FLOW Morikita Publishing Co., Ltd. (2003. 3) pp. 93-96
- (4) A. Serizawa, I. Kataoka and I. Michiyoshi : Turbulence Structure of Air-Water Bubbly Flow— I. Measuring Techniques International Journal of Multiphase Flow (1975. 12) Vol. 2 No. 3 pp. 221-233
- (5) N. Zuber and J. A. Findlay : Average Volumetric Concentration in Two-Phase Flow Systems Journal of Heat Transfer Trans. ASME (1965. 11) Vol. 87 No. 4 pp. 453-468
- (6) M. Ishii : One-Dimensional Drift-Flux Model and Constitutive Equations for Relative Motion Between Phases in Various Two-Phase Flow Regimes ANL-77-47 (1977. 10)
- (7) The Japan Society of Mechanical Engineers (JSME) : JSME STANDARD Guideline for Fluid-elastic Vibration Evaluation of U-bend Tubes in Steam Generators JSME S016 (2002. 3) p. B80